Wind and Structures, Vol. 14, No. 2 (2011) 113-131
DOI: http://dx.doi.org/10.12989/was.2011.14.2.113

Reliability of structures with tuned mass dampers under wind-induced motion: a serviceability consideration

A. Pozos-Estrada, H.P. Hong* and J.K. Galsworthy

Department of Civil and Environmental Engineering, University of Western Ontario, Canada N6A 5B9
(Received October 1, 2009, Accepted July 30, 2010)

Abstract. Excessive wind-induced motion in tall buildings can cause discomfort, affect health, and disrupt the daily activities of the occupants of a building. Dynamic vibration absorbers such as the tuned mass dampers (TMDs) can be used to reduce the wind-induced motion below a specified tolerable serviceability limit state (SLS) criterion. This study investigates whether the same probability of not exceeding specified wind-induced motion levels can be achieved by torsionally sensitive structures without/with linear/nonlinear TMDs subjected to partially correlated wind forces, if they are designed to just meet the same SLS criterion. For the analyses, different structures and the uncertainty in the response, wind load and perception of motion is considered. Numerical results indicate that for structures that are designed or retrofitted without or with optimum linear TMDs and satisfying the same SLS criterion, their probability of exceeding the considered criterion is very consistent, if the inherent correlation between the wind forces is considered in design. However, this consistency deteriorates if nonlinear TMDs are employed. Furthermore, if the correlation is ignored in the design, in many cases a slightly unconservative design, as compared to the designed by considering correlation, is achieved.

Keywords: tuned mass dampers; torsional response; probabilistic analysis; limit state function, serviceability limit state.

1. Introduction

Buildings are designed for life safety and to sustain large horizontal loads, including those caused by strong winds. The buildings could be susceptible to wind loading resulting in excessive vibrations, which could cause discomfort, affect health and disrupt the daily activities of the occupants of a building (Isyumov 1995, Mendis *et al*. 2007). Several authors have studied human perception to vibrations and, proposed guidelines to aid the designers in modifying designs to reduce the wind-induced responses of tall buildings below a serviceability limit state (SLS) (Vickery *et al*. 1983, Isyumov 1995). More recently, studies on the effects of wind-induced building motion on occupant comfort were reported by Tamura (2006), Burton (2006), Burton *et al*. (2006), and Kim and Kanda (2008).

However, due to the complexity and economical constraints, in many cases an extensive structural modification to the new or existing structures is not feasible, and use of active and passive energy

* Corresponding Author, Professor, E-mail: hongh@eng.uwo.ca

dissipation devices, such as tuned mass dampers (TMDs), to reduce the amplitude of the wind-induced vibration is desirable (Kareem *et al*. 1999). A successful application of the TMD system can reduce the amplitude of the vibration below specified tolerable serviceability criteria.

The serviceability criteria are considered in the design to ensure the comfort, health, and continuity of daily activities of the occupants of a building. The design codes and their commentaries recommend sets of load and resistance factors to be used in ultimate and serviceability limit states. The SLS is often focused on the deflections, plumbness and accelerations. Furthermore, the use of energy dissipation devices helps to reduce the wind-induced response of the structure to acceptable levels specified by the SLS. Since wind loading is a stochastic process, structural properties are uncertain and perception levels of motions differ from person to person, it is desirable to study the impact of these uncertainties on the structural responses and to assess whether structures without or with TMDs that are designed to just meet a specified SLS criterion have the same reliability level (i.e., the probability of not exceeding an adopted SLS criterion).

The main objective of this study is to carry out parametric analyses of torsionally sensitive structures without or with TMDs to determine their reliabilities, if the structures are designed to just meet an adopted SLS criterion. Such a study is needed to substantiate whether consistent reliability levels are achieved by structures designed or retrofitted without or with TMDs to just meet a SLS criterion. For the analysis, the uncertainty in the wind characteristics, the perception levels of motion and the peak structural acceleration is considered. The use of linear and nonlinear damping mechanisms in the TMDs and correlation between wind forces are also considered.

2. Wind-induced responses of torsionally sensitive structures without or with TMDs

2.1 Simplified structural modeling

First, consider that the structure is modeled as a generalized two-degree-of-freedom (2DOF) system (lateral displacement Y and rotational displacement θ) with mass M_S, and mass moment of inertia $M_S r_g^2$, as shown in Fig. 1(a). The equation of motion of the asymmetric structure under wind loading can be written as (Hart and Wong 2000)

$$\begin{Bmatrix} \ddot{Y} \\ \ddot{\theta} r_g \end{Bmatrix} + 2\xi\omega_s \begin{bmatrix} 1 & e/r_g \\ e/r_g & \eta_\theta \end{bmatrix} \begin{Bmatrix} \dot{Y} \\ \dot{\theta} r_g \end{Bmatrix} + \omega_s^2 \begin{bmatrix} 1 & e/r_g \\ e/r_g & \eta_\theta^2 \end{bmatrix} \begin{Bmatrix} Y \\ \theta r_g \end{Bmatrix} = \begin{Bmatrix} F_{YN}(t) \\ F_{\theta N}(t) \end{Bmatrix} \tag{1}$$

where ξ is the damping ratio which is assumed to be the same for the two vibration modes, ω_s is the natural frequency in the Y-direction; η_θ is the ratio between the natural frequency in the θ-direction to that of the Y-direction; e is the eccentricity defined as the distance between the center of mass and the center of rotation of the structure; r_g is the radius of gyration; $F_{YN}(t)$ and $F_{\theta N}(t)$ represent, respectively, the scaled horizontal force (i.e., force per unit mass) and the scaled torsional moment (i.e., torsional moment per unit of $M_S r_g$) due to fluctuating wind loading that will be discussed in the next section; and each overdot denotes one temporal differentiation.

Now, consider that the structure shown in Fig. 1(a) is fitted with two TMDs as shown in Fig. 1(b). The use of two eccentric TMDs is aimed at reducing the peak lateral and torsional responses of the structure. Based on the dynamic equilibrium of the coupled structure and the TMDs system

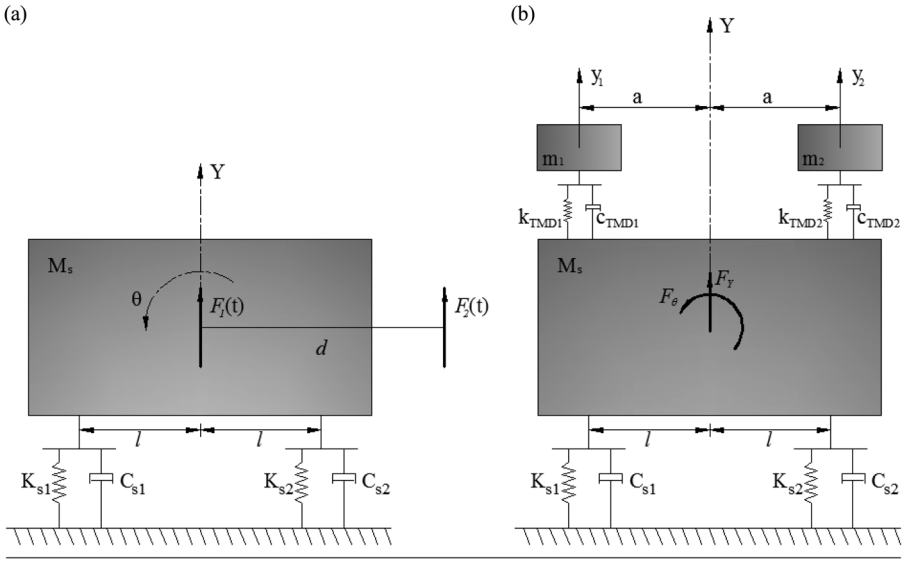

Fig. 1 TMD-structure interaction system

shown in Fig. 1(b), the equation of motion of the TMD-structure system can be established. By simple algebraic manipulation and expressing the properties of the TMDs in terms of the main structure, the equation can be expressed as

$$\{\ddot{X}(t)\} + \{F_{DT}(\dot{X}(t))\} + [K']\{X(t)\} = \{F'(t)\} \tag{2a}$$

where the (scaled) stiffness matrix $[K']$, the displacement vector $\{X(t)\}$, the (scaled) wind-induced force vector $\{F'(t)\}$, and the velocity dependent force vector per unit mass $\{F_{DT}(\dot{X}(t))\}$ are given by

$$[K'] = \omega_s^2 \begin{bmatrix} 1+\mu r_f^2 & e/r_g & -\mu r_f^2/2 & -\mu r_f^2/2 \\ e/r_g & \eta_\theta^2+\mu r_f^2 & a\mu r_f^2/2r_g & -a\mu r_f^2/2r_g \\ -r_f^2/2 & ar_f^2/2r_g & r_f^2/2 & 0 \\ -r_f^2/2 & -ar_f^2/2r_g & 0 & r_f^2/2 \end{bmatrix} \tag{2b}$$

$$\{X(t)\} = \{Y \quad \theta r_g \quad y_1 \quad y_2\}^T \tag{2c}$$

$$\{F'(t)\} = \{F_{YN}(t) \quad F_{\theta N}(t) \quad 0 \quad 0\}^T \tag{2d}$$

and

$$\{F_{DT}(\dot{X}(t))\} = \begin{bmatrix} 2\xi\omega_s(\dot{Y}+\dot{\theta}) + \frac{1}{M_s}F_{D1}(\dot{Y}-a\dot{\theta}-\dot{y}_1) + \frac{1}{M_s}F_{D2}(\dot{Y}+a\dot{\theta}-\dot{y}_2) \\ 2\xi\omega_s\left(\frac{e}{r_g}\dot{Y}+\eta_\theta r_g\dot{\theta}\right) - \frac{a}{M_s r_g}F_{D1}(\dot{Y}-a\dot{\theta}-\dot{y}_1) + \frac{a}{M_s r_g}F_{D2}(\dot{Y}+a\dot{\theta}-\dot{y}_2) \\ -\frac{2}{\mu M_s}F_{D1}(\dot{Y}-a\dot{\theta}-\dot{y}_1) \\ -\frac{2}{\mu M_s}F_{D2}(\dot{Y}-a\dot{\theta}-\dot{y}_2) \end{bmatrix} \quad (2e)$$

In the above equations, μ denotes the ratio of the mass of the TMDs to that of the structure; r_f denotes the ratio of the frequency of the TMDs to the modal frequency of the structure that reduces the structural response to the maximum; $F_{\mathrm{Di}}(v_r)$, i = 1,2, represents the relative velocity dependent damping force of the i-th mass damper; and a is defined as shown in Fig. 1(b). In this study, μ is set equal to 1%, and the optimum value of r_f is selected for design and installation of the TMDs in all cases, where the "optimum" refers to the optimum tuning of the TMD parameters to effectively reduce vibration (Den Hartog 1956, Warburton 1982). The optimum TMDs were obtained based on grid search techniques; this technique is discussed in detail in Vanderplaats (1984) and is justified since no closed form solution is available for the type of excitations and TMD-structure system analyzed. In formulating Eq. (2), it is considered that the same type of dampers is to be installed in the structure, and that one is interested in mitigating the vibration caused by the fluctuating wind pressure (Simiu and Scanlan 1996). This assumption is in agreement with typical applications.

Two commonly used functional forms to represent the damping force in the TMDs system are considered in this study. One is used to represent the viscous damping force which is considered to be proportional to the relative velocity, v_r, given by

$$F_D(v_r) = C_L v_r \quad (3)$$

where C_L denotes viscous damping coefficient. The other is of the power law type which allows a simple representation of a nonlinear damping force (Vickery *et al*. 2001) expressed as

$$F_D(v_r) = C_{PL} sign(v_r)|v_r|^{\beta} \quad (4)$$

where C_{PL} is a power law damping coefficient; $|\bullet|$ denotes the absolute value of its argument and β is a power law exponent which is set equal to 2 in this study.

2.2 Wind loading model

Temporally and spatially varying wind pressures acting on a structure could produce the along-wind force and torsional moment, which could be modeled by the combination of two uncorrelated stochastic processes. More specifically, it is considered that the scaled along-wind force $F_{YN}(t)$ and the scaled wind-induced torsional moment $F_{\theta N}(t)$ can be modeled by the combination of two uncorrelated stochastic processes $F_1(t)$ and $F_2(t)$ (see Fig. 1(a)) given by

$$F_{YN}(t) = c\sqrt{1-\rho_{F_YF_\theta}{}^2}F_1(t) + \rho_{F_YF_\theta}cF_2(t) \tag{5a}$$

and

$$F_{\theta N}(t) = (R/r_g) \times (\rho_{F_YF_\theta}cF_2(t)) \tag{5b}$$

where c is a scaling factor that is explained below and takes into account the air density ρ, wind drag coefficient C_D, area of exposure A_e, mean wind speed v, turbulence intensity I_v, and the mass of structure M_s; and R measures the distance from the torsional center to the line of the eccentric force ($\rho_{F_YF_\theta}cF_2(t)$). It can be shown that $\rho_{F_YF_\theta}$ in Eq. (5) represents the correlation coefficient between $F_{YN}(t)$ and $F_{\theta N}(t)$. If the variance of $F_1(t)$ and $F_2(t)$ are normalized to be equal to one, the standard deviations of $F_{YN}(t)$ and $F_{\theta N}(t)$, denoted by $\sigma_{F_{YN}}(v)$ and $\sigma_{F_{\theta N}}(v)$, are equal to c and $(R/r_g)\rho_{F_YF_\theta}c$, respectively, where c for a designed structure can be expressed as

$$c = \left(\frac{\rho C_D A_e v^2}{M_s}\right) I_v \tag{6a}$$

Use of the wind loading model shown in Eq. (5) for the parametric investigations is advantageous since it can be used to cope with ranges of load eccentricities and correlation coefficients between $F_{YN}(t)$ and $F_{\theta N}(t)$.

The considered power spectral density (PSD) function of $F_1(t)$ and $F_2(t)$ for this study is given, as a function of the frequency f, by $S(f)$ which is proportional to $f^{-(1+\alpha)}$ and to the power of v in the frequency range of 0.05 to 0.5 (Hz) and equal to 0 outside this range, α is a model parameter set equal to 1.5. The adoption of such a PSD function is justified since tests at the Boundary Layer Wind Tunnel Laboratory of the University of Western Ontario indicate that such a PSD function provides sufficient accurate characterization of the fluctuating wind force in the inertial subrange, which is of interest in the present study. If the proportionality of $S(f)$ to the power of v is lumped into Eq. (6a)

$$c = \left(\frac{\rho C_D A_e v^\gamma}{M_s}\right) I_v \tag{6b}$$

where γ ranges typically from 2.2 to 2.6 according to the approximation of the upper tail of the PSD of the wind forces of interest, the PSD becomes $S(f) = Af^{-(1+\alpha)}$, where A is a normalization constant such that the integration of the PSD function equals one.

Samples of time-history of $F_1(t)$ and $F_2(t)$ can be obtained based on their PSD functions and using simulation algorithms (Shinozuka 1972, Di Paola 1998, Kareem 2008). For simplicity, the approach given by Shinozuka (1972) is adopted in the presented study. The simulated time series of $F_1(t)$ and $F_2(t)$ can be substituted into Eq. (5) to obtain samples of $F_{YN}(t)$ and $F_{\theta N}(t)$, which can then be used in Eqs. (1) or (2) to calculate the response time history of the structure without or with the TMD system by using the Newmark method.

2.3 Peak responses

2.3.1 Structures without TMDs

Probabilistic characterization of the responses of the structure shown in Fig. 1(a) is needed to estimate the probability that the wind-induced motion exceeds the SLS criterion that is recommended by a design code or prescribed by building owner(s). For this characterization, it is considered that

the structure satisfies the ultimate limit state (ULS) requirements and that the structure is also designed to just meet a SLS criterion defined based on the wind-induced motion, which is to be evaluated using 10-year return period value of the (mean) wind speed, v_{10}, as specified by the NBCC (2005).

The wind-induced response of interest is the mean of the total peak translational acceleration $\hat{\ddot{Y}}$ that is defined by

$$\hat{\ddot{Y}} = \max_{t \in [0, T_d]} \left| \ddot{Y}(t) \pm r\ddot{\theta}(t) \right| = \max_{t \in [0, T_d]} \left| \ddot{Y}(t) \pm (r/r_g) \times \ddot{\theta}(t) r_g \right| \tag{7}$$

where T_d is the duration of the time history of the responses which is set equal to 3600 s, and r is the distance from the point of interest within the structural footprint to the torsional center. Note that Eq. (7) considers the contribution of both the torsional acceleration and translational acceleration. This consideration can be justified since the torsional acceleration experienced away from the torsional center is felt by the inhabitants of a building as a translational motion (Burton 2006, ISO 2631-1 1997).

The direct application of the gust factor approach (Davenport 1964) may not be feasible for estimating the mean peak response defined in Eq. (7), which depends on both translational and rotational responses. To overcome this, one could carry out time-history analyses mentioned earlier to obtain enough samples of $\hat{\ddot{Y}}$, which can be used to establish the probabilistic characterization of $\hat{\ddot{Y}}$ and to estimate the mean of $\hat{\ddot{Y}}$.

Since the structure is modeled as a linear system, the response $\hat{\ddot{Y}}$ is simply equal to $c\hat{\ddot{Y}}_{c=1}$ where $\hat{\ddot{Y}}_{c=1}$ represents the response of the system $\hat{\ddot{Y}}$ for when c shown in Eq. (5) is equal to 1.0. This is advantageous for the parametric study, because $\hat{\ddot{Y}}_{c=1}$ is independent of the parameters of the designed structure and the mean wind speed that is used to define c as shown in Eqs. (5) and (6), and the statistics of the response for any given mean wind speed can be obtained by scaling $\hat{\ddot{Y}}_{c=1}$. Furthermore, the correspondence between a structure that is designed to just meet the SLS criterion under wind excitations, and the associated design wind loading (for SLS) can be established through the parameter c.

Given values of $\rho_{F_Y F_\theta}$, R/r_g, $S(f)$ and characteristics of the structure, the evaluation of a sample of $\hat{\ddot{Y}}_{c=1}$ can be carried out by: simulating $F_1(t)$ and $F_2(t)$; evaluating $F_{YN}(t)$ and $F_{\theta N}(t)$ using Eq. (5); solving Eq. (1) using the Newmark method; and finding $\hat{\ddot{Y}}_{c=1}$ using Eq. (7) and the response time history. Samples of $\hat{\ddot{Y}}_{c=1}$ together with a value of c are used in assessing the mean of $\hat{\ddot{Y}}$, $m_{\hat{\ddot{Y}}}$, and the standard deviation of $\hat{\ddot{Y}}$, $\sigma_{\hat{\ddot{Y}}}$, or to fit the Gumbel probability model (Davenport 1964).

To define the probabilistic model of $\hat{\ddot{Y}}$ by considering different mean wind speeds, let $\hat{\ddot{Y}}(v_{10})$ denote the peak response evaluated based on 10-year return period (mean) wind speed v_{10}. It can be shown that if the design requires that the mean of $\hat{\ddot{Y}}(v_{10})$ for the designed structure equals a specified value a_{cr}

$$a_{cr} = E(\hat{\ddot{Y}}(v_{10})) \tag{8a}$$

where $E(\ )$ denotes the expectation, the mean peak response conditioned on the mean wind speed v is simply equal to,

$$E(\hat{\ddot{Y}} \,|\, v) = \left(\frac{v}{v_{10}}\right)^{\gamma} E(\hat{\ddot{Y}}(v_{10})) \tag{8b}$$

provided that the wind drag coefficient C_D and the turbulence intensity I_v can be treated as independent of the value of the mean wind speed v. Experience indicates that in many practical applications the partial correlation between the along-wind force and the torsional moment are not taken into account in evaluating the total mean peak response due to different vibration modes. It is of interest to estimate the adequacy of a structure that is designed by ignoring this correlation. This leads to that the mean of $\hat{\ddot{Y}}_0(v_{10})$ equals a_{cr}

$$a_{cr} = E(\hat{\ddot{Y}}_0(v_{10})) \tag{9a}$$

where $\hat{\ddot{Y}}_0(v_{10})$ denotes the peak response evaluated based on 10-year return period (mean) wind speed v_{10} but ignoring any possible correlation between of $F_{YN}(t)$ and $F_{\theta N}(t)$. In such a case, Eq. (8b) can be conveniently written as

$$E(\hat{\ddot{Y}} \,|\, v) = \left(\frac{v}{v_{10}}\right)^{\gamma} R_{\gamma} E(\hat{\ddot{Y}}_0(v_{10})) \tag{9b}$$

where $R_\gamma = E(\hat{\ddot{Y}}_0(v_{10}))/E(\hat{\ddot{Y}}_0(v_{10}))$ represents the ratio of the expected value of the peak acceleration evaluated at v_{10} by considering the correlation to that by ignoring the correlation. Eq. (9b) effectively relates $E(\hat{\ddot{Y}} \,|\, v)$ to the design requirement shown in Eq. (9a) (i.e., $E(\hat{\ddot{Y}} \,|\, v) = (v/v_{10})^{\gamma} R_\gamma a_{cr}$).

To estimate the performance of the design under serviceability consideration, we define the normalized mean wind speed, V_n, $V_n = V/v_{10}$, where V denotes the annual maximum wind speed. By adopting the Gumbel probability model (Davenport 1964) and using Eqs. (8) and (9), the probability density function of $\hat{\ddot{Y}}$ conditioned on the value of V_n, v_n, is

$$f_{\hat{\ddot{Y}}|V_n}(\hat{\ddot{y}} \,|\, v_n) = \alpha_{\hat{\ddot{Y}}} \exp(-\alpha_{\hat{\ddot{Y}}}(\hat{\ddot{y}} - u_{\hat{\ddot{Y}}}) - \exp(-\alpha_{\hat{\ddot{Y}}}(\hat{\ddot{y}} - u_{\hat{\ddot{Y}}}))), \tag{10}$$

where $f_{\hat{\ddot{Y}}|V_n}(\hat{\ddot{y}} \,|\, v_n)$ is the conditional probability density function, $\delta_{\hat{\ddot{Y}}}$ denotes the coefficient of variation (cov) of $\hat{\ddot{Y}}$, $\alpha_{\hat{\ddot{Y}}} = \pi/(\sqrt{6} v_n^{\gamma} R_Y a_{cr} \delta_{\hat{\ddot{Y}}})$, and $u_{\hat{\ddot{Y}}} = (1 - 0.577\sqrt{6}\delta_{\hat{\ddot{Y}}}/\pi) v_n^{\gamma} R_Y a_{cr}$, in which $R_Y = 1.0$ if Eq. (8a) is considered for design and if Eq. (9a) is employed. Since the annual maximum wind speed is commonly modeled as a Gumbel variate, V_n is a Gumbel variate as well with its cov value equal to that of V, δ_v, and the probability distribution function given by

$$F_{V_n}(v_n) = \exp(-\exp(-\alpha_{v_n}(v_n - u_{v_n}))) \tag{11}$$

in which $\alpha_{v_n} = \pi/(\sqrt{6}\delta_v m_{v_n})$, $u_{v_n} = (1 - 0.577\sqrt{6}\delta_v/\pi) m_{v_n}$, where m_{v_n} is given by

$$m_{v_n} = \left[1 - (0.577 + \ln(-\ln(1 - 1/10))) \times \frac{\sqrt{6}\delta_v}{\pi}\right]^{-1} \tag{12}$$

2.3.2 Structures with TMDs

If the structure is fitted with two optimum TMDs as shown in Fig. 1(b), and the design (with the TMDs) is such that it just meets the SLS criterion, the probabilistic characterization of the response $\hat{\ddot{Y}}$ can also be carried out by using the same procedure as outlined in the previous section for the case of structures without TMDs. However, since the governing equation could contain the

nonlinear damping force, and the response is not linearly related to the parameter c, the design including the TMDs needs to be adjusted such that the specified SLS criterion is just met. Alternatively, to simplify the reliability analysis and without loss of generality, for a designed structure with optimum TMDs, one can adjust the c value iteratively such that the designed structure just meets the SLS criterion. Since c is related to the structural characteristics as indicated in Eq. (6), the adjustment of the value of c for the structure with or without TMDs effectively changes the design to just meet the SLS. The latter is considered for the parametric studies in the present work.

One more significant difference between structures without and with TMDs is that for a structure with nonlinear TMDs, Eqs. (8b) and (9b) are no longer applicable and the cov of $\hat{\ddot{Y}}$ must be evaluated numerically for each given value of V, v. The obtained mean and cov are then used in Eq. (10) to define the parameters of the probability distribution of $\hat{\ddot{Y}}$.

3. Serviceability limit state and reliability analysis

One of the SLS that needs to be considered for the design of tall buildings under wind loading is based on wind-induced motion: peak acceleration or standard deviation of acceleration. Several studies on the human perception of motion have been reported in the literature (Reed 1971, Chen and Robertson 1972, Goto 1975, 1983, Irwin 1979, Kanda *et al*. 1988, Melbourne and Cheung 1988, Kareem 1988, Isyumov 1993, 1995, Tamura 2003, Burton 2006, Burton *et al*. 2006, Tamura *et al*. 2006, Kim and Kanda 2008). In all the mentioned studies, the discomfort level and disruption of tasks of the inhabitants of buildings are related to the mean peak acceleration and/or standard deviation of the acceleration for a given acceleration frequency. Criteria to limit the excessive wind-induced motion were developed and adopted in design codes or their corresponding commentaries as serviceability limit states (e.g., NBCC 2005, AIJ 2004, ISO10137 2007). The criterion in the commentaries to the NBCC (2005) is based on the mean peak acceleration that is to be used to compare the wind-induced motion for a 10-year return period value of the wind speed. This criterion neglects the influence of the structural frequency on the perception threshold of the occupants of the building. The criteria in the ISO10137 (2007) are similar to those suggested in the AIJ (2004) which are based on the mean peak acceleration and are to be used to compare the mean peak acceleration of the structure estimated for a 1-year return period value of wind speed. The criteria in the AIJ (2004), which are considered in this study, depend on the selected probability of perception level as shown in Fig. 2(a). It must be noted that the criteria are to be used to compare the responses obtained based on 1-year return period value of 10-minutes mean wind speed, while the responses calculated according the NBCC (2005) are based on 10-year return period value of mean hourly wind speed. Therefore, to adopt these criteria for serviceability checking, they should be scaled by taking into account the differences in the wind velocities evaluated based on different averaging time, and the differences in the return periods (Pozos-Estrada *et al*. 2010). The scaling from the 1-year return period value to 10-year return period value of hourly mean wind requires a factor of 1.47, which is applicable to typical Canadian sites. The ratio of hourly mean wind speed to 10-minutes mean wind speed equals 0.9 according to the curve given by Durst (1960). These factors lead to the corresponding criteria shown in Fig. 2(b).

It is noteworthy that the percentage of people that can perceive the vibration versus the logarithm of the measured peak acceleration for a given frequency can be approximately fitted with a lognormal

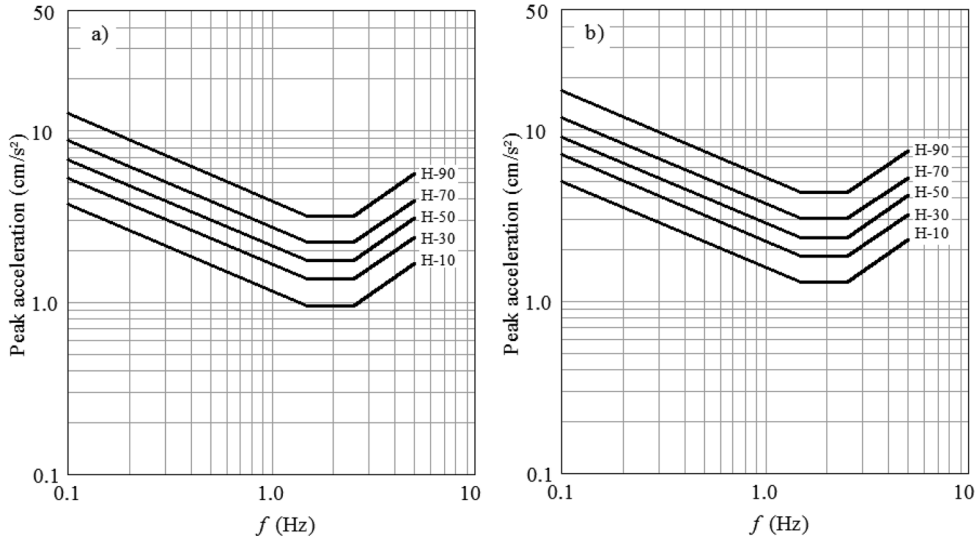

Fig. 2 Serviceability criteria considering 10%, 30%, 50%, 70% and 90% probability of perceiving the vibration (denoted by H10, H30, H50, H70 and H90, respectively): (a) 1-year return period value of 10-minutes mean wind speed (suggested by AIJ 2004); (b) 10-year return period value of 60-minutes mean wind speed (mapped from Fig. 2(a))

distribution function (Chen and Robertson 1972, Tamura *et al*. 2006, Burton 2006). Based on these observations, the percentage of people that can perceive the vibration can be expressed as

$$P_{P|\hat{\ddot{Y}}}(\hat{\ddot{y}}) = \Phi\left(\frac{ln(\hat{\ddot{y}}/c_1)}{c_2}\right) \tag{13}$$

where $P_{P|\hat{\ddot{Y}}}$ is the probability of perception for a given peak acceleration level $\hat{\ddot{y}}$, $\Phi(\bullet)$ is the standard normal distribution function and c_1 and c_2 are model parameters that can be inferred from Burton (2006) and are shown in Table 1 for a range of frequencies. Eq. (13) is used to define the perception level of vibration of the inhabitants of a building in a reliability context in the next section.

To determine the reliability of the structure without or with TMDs (i.e., the probability that the

Table 1 Parameters c_1 and c_2 for Eq. (13) inferred from Burton (2006)

f (Hz)	c_1 (milli-g)[1]	c_2
0.1	4.577	0.792
0.2	3.421	0.773
0.3	2.901	0.782
0.4	2.435	0.826
0.5	2.171	0.861

Note: (1) c_1 and c_2 for f = 0.1 Hz were obtained by extrapolation.

wind-induced structural motion is less than the adopted SLS criterion used in design), one must consider the uncertainty in the wind-induced structural motion, the (mean) wind speed and the probability of motion perception (See Eqs. (10), (11) and (13)). By taking these uncertainties into account, the probability of perception of wind-induced motion by the inhabitants of a building, P_{fP}, can be expressed as

$$P_{fP} = \iint \Phi\left(\frac{\ln(\hat{\ddot{y}}/c_1)}{c_2}\right) f_{\hat{\ddot{Y}}|V_n}(\ddot{y}|v_n) f_{V_n}(v_n)\, dv_n d\ddot{y} \tag{14}$$

where the integration of Eq. (14) is over the domains of V_n and $\hat{\ddot{Y}}$, and can be evaluated using a simple simulation technique.

4. Numerical analysis and results

4.1 Reliability of structures without TMDs

For the parametric analyses, structures subjected to different combinations of wind loading conditions and structural dynamic properties are considered. As explained in Section 2, the main structure is idealized as a 2DOF system whose characteristics are defined by the generalized properties of the actual structure. For the moment, consider that the structure shown in Fig. 1(a) with $\xi = 1\%$, $\omega_Y = 0.787$ rad/s, $\eta_\theta = 0.5$, and $e/r_g = 0$ is subjected to the wind loads defined in Eq. (5) with $\rho_{F_Y F_\theta} = 0$ and $R/r_g = 0.5$, and that the design requires that $E(\hat{\ddot{Y}}(v_{10}))$ equals the H50 criterion, proposed in AIJ (2004) shown in Fig. 2(b). This requirement results in $a_{cr} = 0.0796$ m/s^2 (8.11 milli-g), which is selected based on the greatest vibration frequency between those for sway and torsional vibration modes. The above indicates that the structure is designed such that c equals $a_{cr}/E(\hat{\ddot{Y}}_{c=1})$, where $E(\hat{\ddot{Y}}_{c=1})$ is evaluated for 10-year return period (mean hourly) wind speed, and that possible correlation between wind forces is considered. Note that the same criterion used to select a_{cr} is used to select the corresponding parameters c_1 and c_2 that are needed in defining Eq. (13).

The evaluation of $E(\hat{\ddot{Y}}_{c=1})$ is based on the simulation procedure discussed in Section 2 with a simulation cycle of 100. Samples of $\hat{\ddot{Y}}_{c=1}$ are also used to estimate $S_{\hat{\ddot{Y}}}$ that is needed to characterize the distribution parameters $\hat{\ddot{Y}}$ of as shown in Eq. (10). To verify that the number of simulation cycles is sufficient, the analysis is repeated with a simulation cycle of 200, and the obtained values of $E(\hat{\ddot{Y}}_{c=1})$ are almost identical to those obtained with a simulation cycle of 100 (with a difference less than 2%). Therefore, a simulation cycle of 100 is adopted in the remaining part of this study for estimating $E(\hat{\ddot{Y}}_{c=1})$ or $\delta_{\hat{\ddot{Y}}}$ which is used to characterize Eq. (10).

To estimate the probability of perception of wind-induced motion, a value of δ_v equal to 0.1 is selected since it reflects the wind climate in many Canadian cities. Based on these considerations, Eq. (14) is solved numerically and the calculated value of P_{fP} is shown in Table 2 for γ equal to 2.2. It is observed that the estimated P_{fP} differs from the probability of 50% considered in the H50 criterion. This is expected since the latter did not include the uncertainty in wind-induced responses.

To assess the impact of the correlation between the along-wind and the torsional forces on P_{fP}, $\rho_{F_Y F_\theta}$ is varied from 0 to 1.0 with an increment of 0.25 while maintaining the values of the remaining parameters of the structure to be the same. The obtained P_{fP} values are also depicted in

Table 2 Estimated P_{fP} for $e/r_g = 0$, $R/r_g = 0.5$, $r/r_g = 0.5$, $\delta_{v_n} = 0.1$, and $\gamma = 2.2$

Structure No.	ω_Y (rad/s)	η_θ	$\rho_{F_Y F_\theta}$				
			0	0.25	0.5	0.75	1
1	0.785	0.5	0.684	0.684 (0.688)	0.683 (0.714)	0.681 (0.723)	0.684 (0.747)
2	0.785	1	0.684	0.684 (0.688)	0.681 (0.690)	0.681 (0.722)	0.684 (0.766)
3	0.785	1.5	0.681	0.680 (0.683)	0.679 (0.684)	0.677 (0.672)	0.682 (0.709)
4	0.785	2	0.680	0.679 (0.693)	0.678 (0.684)	0.678 (0.688)	0.681 (0.699)
5	1	0.5	0.681	0.681 (0.703)	0.680 (0.708)	0.680 (0.731)	0.681 (0.749)
6	1	1	0.682	0.681 (0.691)	0.680 (0.700)	0.679 (0.716)	0.681 (0.757)
7	1	1.5	0.628	0.629 (0.625)	0.627 (0.631)	0.627 (0.639)	0.629 (0.655)
8	1	2	0.619	0.620 (0.616)	0.617 (0.608)	0.618 (0.620)	0.620 (0.628)

Note: The values inside brackets were calculated with Eq. (9a).

Table 2, indicating that P_{fP} is not sensitive to $\rho_{F_Y F_\theta}$ for the considered structure if the design is based on the mean peak response estimated by considering such a correlation (i.e., Eq. (8a)).

The above analysis was repeated but considering structures with different ω_r and η_θ values. For each structure, a_{cr} was taken from the H50 criterion shown in Fig. 2(b). The estimated P_{fP} values are shown in Table 2 as well. It is observed from the table that P_{fP} is very consistent for the structures considered.

To see the effect of adopting Eq. (9a) for design on P_{fP}, designs for the cases shown in Table 2 are carried out according to Eq. (9a) rather than Eq. (8a), and the above analyses are repeated. The obtained P_{fP} values are compared with those obtained for designs based on Eq. (8a) in Table 2. The comparison of the results suggests that, in general, an increase in the correlation between the along-wind force and the torsional moment have the effect of increasing P_{fP}, if the structure is designed to satisfy Eq. (9a). This increase is more significant if the along-wind force and the torsional moment are fully correlated. This implies that in most cases, a slightly unconservative design is achieved by ignoring the correlation between the along-wind force and the torsional moment.

To investigate the impact of the parameters e/r_g, R/r_g, r/r_g and δ_v on P_{fP}, Structures 1 and 4 presented in Table 2 are re-analyzed, and the obtained values of P_{fP} by considering the design criterion shown in Eq. (8a) are depicted in Fig. 3. The figure shows that the use of 10-year return period value of the wind speed and the same a_{cr} for limiting the wind-induced motions does not ensure the same P_{fP} for regions having different δ_v values. For regions with higher δ_v values, P_{fP} is decreased, which is expected since a larger S_v leads to a greater 10-year return period wind speed for design. It is also observed from the figure that e/r_g, R/r_g and r/r_g do not significantly impact P_{fP}, and that P_{fP} is very consistent, which was already observed in Table 2.

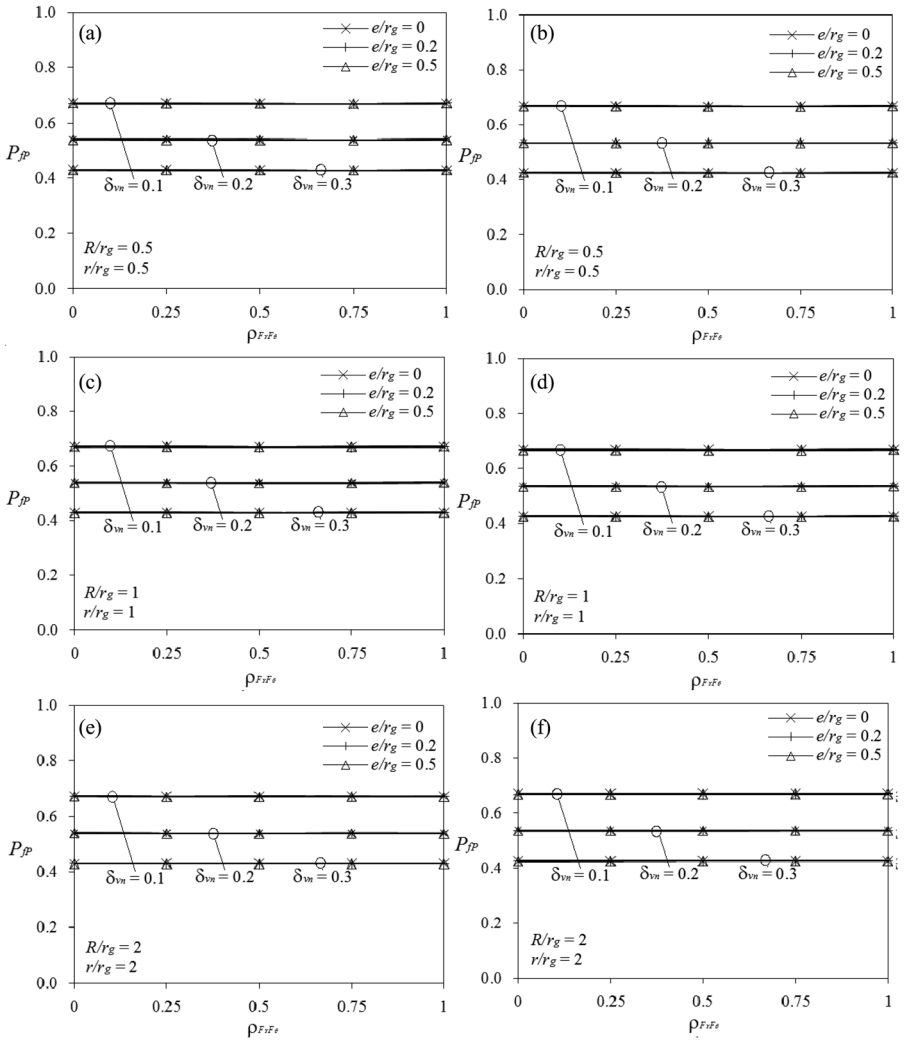

Fig. 3 Calculated P_{fP} considering the H50 criterion from AIJ ((a), (c) and (e) are for Structure 1, and (b), (d) and (f) are for Structure 4)

To investigate the influence of the adopted SLS criterion on P_{fP}, the H90 criterion instead of the H50 criterion is employed for the design checking (i.e., a_{cr} selected from the H90 is used for design), and the above analyses are repeated. The results are shown in Fig. 4. Comparison of the results shown in Figs. 3 and 4 indicates that similar conclusions to those drawn from Fig. 3 are applicable to Fig. 4.

The above analyses were carried out again for the cases shown in Table 2, but considering γ equal to 2.4 and 2.6, the estimated P_{fP} values are similar to those for γ equal 2.2 and for that reason they are not shown.

It is acknowledged that P_{fP} is likely to be affected by the uncertainty in vibration frequency and damping ratio of the structure. Consideration of these uncertainties that could be important is outside of the scope of the present study.

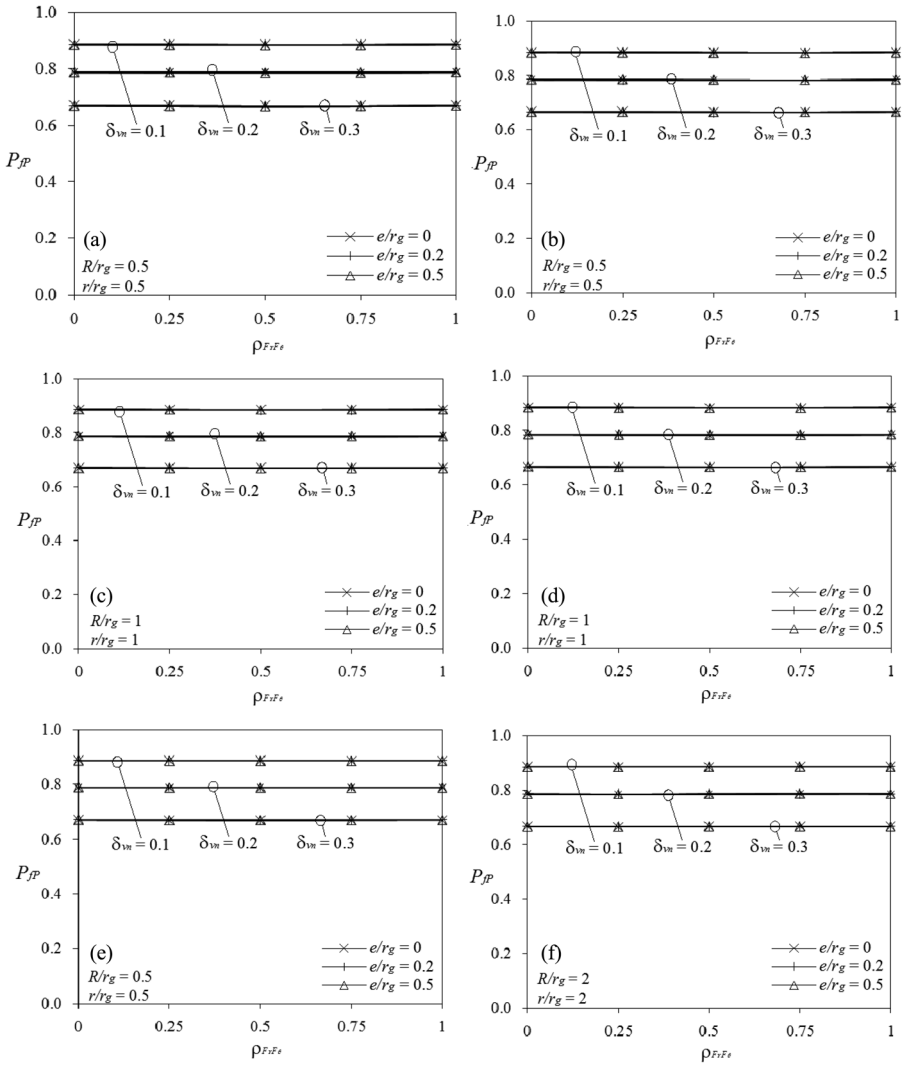

Fig. 4 Calculated values of P_{fP} considering the H90 criterion from AIJ ((a), (c) and (e) are for Structure 1, and (b), (d) and (f) are for Structure 4)

4.2 Reliability of structures with TMDs

4.2.1 Reliability of structures with linear TMDs

Consider that structures with different geometric shapes, located at different regions, and having the same vibration frequencies and damping ratios to those considered in the previous section need to be constructed or retrofitted with optimum TMDs to reduce wind-induced motions.

First, consider that the main structure with ξ = 1%, ω_Y = 0.787 rad/s, η_θ = 0.5, and e/r_g = 0 is fitted with two optimum linear TMDs, as illustrated in Fig. 1(b), with mass ratio μ equal to 1% and the optimum frequency ratio and coefficient of damping, as a function of the coefficient of damping

of the main structure (i.e., $C_s = 2\xi\omega_Y M_s$), shown in Table 3, which were calculated based on a grid search technique. The structures with TMDs are to be checked such that $E(\hat{\ddot{Y}}(v_{10}))$ equals a_{cr} that is dictated by the H50 criterion (Fig. 2(b)). This checking or design criterion was expressed in Eq. (8a).

If the main structure is subjected to the wind loads defined in Eq. (5) with $\delta_v = 0.1$, $R/r_g = 0.5$, and a value of c that leads to Eq. (8a) to be satisfied, by using the characteristics of the TMD-structure system and the parameters of the wind loading model, Eq. (2a) is solved numerically and the total peak translational acceleration is calculated by using Eq. (7) for $r/r_g = 0.5$. By considering this information, and similar to the case of the structures without TMDs, Eq. (14) is solved numerically and the calculated P_{fP} values are shown in Table 4 for γ equal to 2.2. Furthermore, results are calculated and presented in Table 4 for the same TMD-structure system but considering different combinations of ω_Y, η_θ, and e/r_g for the main structure, $\rho_{F_Y F_\theta}$ and R/r_g for the wind loading, and r/r_g. A comparison of results shown in Tables 2 and 4 indicates that the reliability of structures without and with linear TMDs is almost identical for the cases considered. It implies that the same safety level is achieved whether the design is without or with the installation of the optimum linear TMDs if the same serviceability criterion to limit the wind-induced vibration is used for checking. Therefore, identical serviceability criteria can be used for the design or retrofitting structures without or with optimum linear TMDs to meet the same tolerable probability of motion perception levels.

Again, if the design is carried out according to Eq. (9a) rather than Eq. (8a), by repeating the above analysis, for the cases shown in Table 4, the obtained P_{fP} values are shown in Table 4 as well. A comparison of Tables 2 and 4 reveals that the calculated P_{fP} values are different for structures without or with linear TMDs if Eq. (9a) is used for design. This indicates that if the correlation is ignored in design, its effect on the estimated P_{fP} differs for structures without and with TMDs. However, in general, the difference is small, and a slightly unconservative design is achieved in most cases by ignoring the correlation between the along-wind force and torsional moment.

A further analysis is carried out by considering Structures 1 and 4, which are fitted with optimum linear TMDs. The obtained P_{fP} values by considering the H50 criterion, and Eq. (9a) are shown in Fig. 5 for several combinations of e/r_g, R/r_g, r/r_g and δ_v. The figure indicates that P_{fP} is not

Table 3 Optimum parameters of the TMDs

Structure No.	ω_Y (rad/s)	η_θ	Linear TMDs		Nonlinear TMDs	
			r_{fopt}	C_{opt}/C_S	r_{fopt}	C_{opt}/C_S (m/s)$^{-1}$
1	0.785	0.5	0.5	0.03	0.5	0.075
2	0.785	1	1	0.06	1	0.11
3	0.785	1.5	1.05	0.158	1	0.15
4	0.785	2	1	0.07	1	0.15
5	1	0.5	0.5	0.025	0.5	0.075
6	1	1	1	0.06	1	0.12
7	1	1.5	1	0.08	1	0.15
8	1	2	1	0.06	1	0.15

Table 4 Estimated P_{fP} for $e/r_g = 0$, $R/r_g = 0.5$, $r/r_g = 0.5$, $\delta_{v_n} = 0.1$, and $\gamma = 2.2$ for the structure with linear TMDs

Structure No.	ω_Y (rad/s)	η_θ	$\rho_{F_Y F_\theta}$				
			0	0.25	0.5	0.75	1
1	0.785	0.5	0.684	0.684	0.684	0.683	0.685
				(0.697)	(0.709)	(0.720)	(0.759)
2	0.785	1	0.684	0.683	0.680	0.681	0.684
				(0.691)	(0.708)	(0.725)	(0.776)
3	0.785	1.5	0.681	0.680	0.679	0.679	0.681
				(0.686)	(0.673)	(0.672)	(0.709)
4	0.785	2	0.682	0.680	0.679	0.678	0.681
				(0.693)	(0.692)	(0.684)	(0.707)
5	1	0.5	0.682	0.682	0.679	0.681	0.682
				(0.692)	(0.702)	(0.716)	(0.747)
6	1	1	0.682	0.682	0.680	0.680	0.682
				(0.696)	(0.705)	(0.744)	(0.777)
7	1	1.5	0.629	0.628	0.628	0.627	0.629
				(0.633)	(0.638)	(0.641)	(0.660)
8	1	2	0.620	0.620	0.618	0.619	0.620
				(0.615)	(0.618)	(0.611)	(0.645)

Note: The values inside brackets were calculated with Eq. (9a).

sensitively affected by $\rho_{F_Y F_\theta}$ as long as such a consideration is taken into account in design, and that changes in e/r_g, R/r_g and r/r_g do not impact the calculated P_{fP} values. Results by using H90 instead of H50 are also calculated. As the trends that can be observed from these results are similar to those observed from Fig. 5, the results for H90 are not shown.

The above analyses were repeated but considering γ equal to 2.4 and 2.6. Again, the results indicate that P_{fP} is not very sensitive to the considered γ values.

4.2.2 Reliability of structures with nonlinear TMDs

To investigate possible effects of the use of optimum nonlinear TMDs on P_{fP}, analyses are carried out for a subset of TMD-structure systems considered in the previous section. The parameters of the nonlinear TMDs with μ equal to 1% are shown in Table 3. Similar to the case of structures with linear TMDs, the structures with nonlinear TMDs are to be checked using Eq. (8a) and the corresponding a_{cr} values, which is dictated by the H50 criterion. By following the same procedure used in the previous section, the obtained P_{fP} values are shown in Table 5, and Fig. 6 for selected values of e/r_g, R/r_g, r/r_g, δ_v and $\rho_{F_Y F_\theta}$. The conclusions and observations that can be drawn from the table and figures are similar to those for structures with linear TMDs. However, P_{fP} for structures with nonlinear TMDs is greater than those obtained for structures without or with optimum linear TMDs. This implies that more stringent serviceability criterion is required to limit the wind-induced vibration if the optimum nonlinear TMDs with the considered nonlinear behaviour is used in design. This observation needs to be investigated further by considering nonlinear TMDs with different

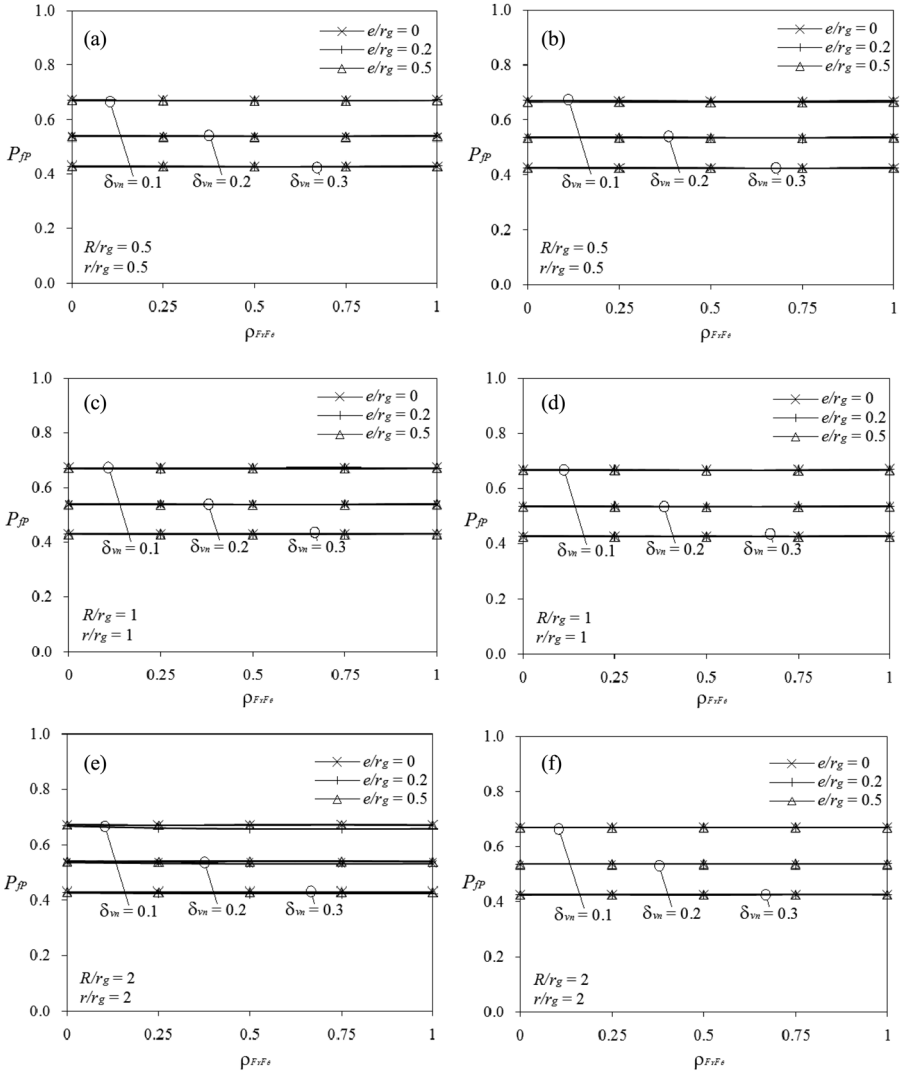

Fig. 5 Calculated values of P_{fP} considering the H50 criterion from AIJ ((a), (c) and (e) are for Structure 1 fitted with linear TMDs, and (b), (d) and (f) are for Structure 4 fitted with linear TMDs)

nonlinear characteristics. Again, as in the case of structures fitted with optimum linear TMDs, the results by using H90 instead of H50 are also calculated. The conclusions that can be drawn from the results are similar to those drawn from Fig. 6, and for that reason the results for H90 are not shown.

If Eq. (9a) is employed for design, the estimated P_{fP} values with optimum nonlinear TMDs are shown in Table 5. Again, the observations from this table are similar to those from Tables 2 and 4, and that unconservative design is achieved in all the considered cases if the correlation between the wind forces is ignored for SLS design checking. Furthermore, analysis results showed that these P_{fP} values are insensitive to γ ranging from 2.2 to 2.6.

Table 5 Estimated P_{fP} for $e/r_g = 0$, $R/r_g = 0.5$, $r/r_g = 0.5$, $\delta_{v_n} = 0.1$, and $\gamma = 2.2$ for the structure with nonlinear TMDs

Structure No.	ω_Y (rad/s)	η_θ	$\rho_{F_Y F_\theta}$		
			0	0.5	1
1	0.785	0.5	0.845	0.839	0.796
				(0.843)	(0.834)
2	0.785	1	0.863	0.851	0.803
				(0.860)	(0.852)
3	0.785	1.5	0.819	0.808	0.799
				(0.817)	(0.815)
4	0.785	2	0.813	0.809	0.793
				(0.812)	(0.808)

Note: The values inside brackets were calculated with Eq. (9a).

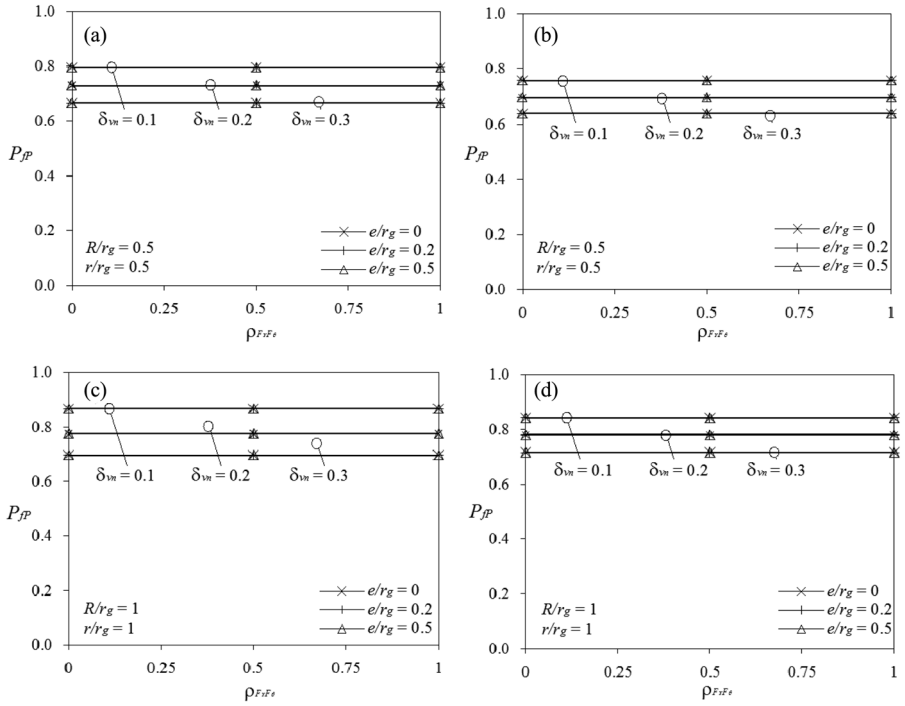

Fig. 6 Calculated values of P_{fP} considering the H50 criterion from AIJ ((a), (c) and (e) are for Structure 1 fitted with nonlinear TMDs, and (b), (d) and (f) are for Structure 4 fitted with nonlinear TMDs)

5. Conclusions

A parametric study was carried out to assess whether consistent reliability levels can be achieved for structures designed or retrofitted without or with TMDs to just meet SLS criteria under wind-induced motion. For the analysis, translation and torsional motion and, linear and nonlinear TMDs are considered. Numerical results suggest that for structures that are designed or retrofitted without

or with optimum linear TMDs and satisfying the same serviceability limit state (SLS) criterion, their probability of exceeding the criterion, P_{fP}, is very consistent, if the inherent correlation between wind forces is taking into account in design. This consistency is advantageous since the same SLS criterion can be adopted in designing or checking the structures without or with TMDs. However, if the optimum tuned nonlinear TMDs with the considered nonlinear behaviour are used, more stringent serviceability criterion than that used for structures without TMDs is required to limit the wind-induced vibration and to achieve a consistent reliability level (i.e., 1-P_{fP}). Other observations that can be drawn from the results include:

1) Uncertainties in peak acceleration $\hat{\ddot{Y}}$ and time-averaged velocity V need to be incorporated in evaluating P_{fP} for wind-induced motion since the estimated probability is significantly different if these uncertainties are considered or ignored; and

2) A slightly unconservative design is achieved in most cases if the correlation between the along-wind force and torsional moment is ignored in SLS design checking.

Acknowledgements

The financial supports of the National Council on Science and Technology (CONACYT) of Mexico, the University of Western Ontario and the National Science and Engineering Research Council (NSERC) are gratefully acknowledged. We are grateful to Dr. P. Irwin for his insightful comments and suggestions.

References

Architectural Institute of Japan Recommendations (2004), "Guidelines for the evaluation of habitability to building vibration", AIJES-V001-2004, Tokyo, Japan.

Burton, M.D. (2006), "Effects of low frequency wind-induced building motion on occupant comfort", PhD. Thesis, Civil Engineering Department, The Hong Kong University of Science and Technology, Hong Kong.

Burton, M.D., Kwok, K.C.S., Hitchcock, P.A. and Denoon, R.O. (2006), "Frequency dependence of human response to wind-induced building motion.", *J. Struc. Eng - ASCE*, **132**(2), 296-303.

Chen, P.W. and Robertson, L.E. (1972), "Human perception thresholds of horizontal motion." *J. Struc. Div - ASCE*, **98**(8), 1681-1695.

Davenport, A.G. (1964), "Note on the distribution of the largest value of a random function with application to gust loading" *Proceedings of the Institution of Civil Engineers*, 28, Paper No. 6739.

Den Hartog, J.P. (1956), *Mechanical Vibrations*, McGraw-Hill, New York.

Di Paola, M. (1998), "Digital simulation of wind field velocity", *J. Wind Eng. Ind. Aerod.,* **74-76**, 91-109.

Durst, C.S. (1960), "Wind speeds over short periods of time", *Meteorol. Mag.,* **89**(1), 056.

Goto, T. (1975), "Research on vibration criteria from the viewpoint of people living in high-rise buildings. (Part 1) Various responses of humans to motion" *Tran. Arch. Inst. Japan,* **237**(11), 109-118.

Goto, T. (1983), "Studies on wind-induced motion of tall buildings based on occupants' reaction", *J. Wind Eng. Ind. Aerod.*, **13**(1-3), 241-252.

Hart, G.C. and Wong, K. (2000), *Structural Dynamics for Structural Engineers*, John Wiley & Sons Inc., New York.

International Organization for Standardization (1997), "Mechanical vibration and shock – Evaluation of human exposure to whole-body vibration – Part I: General requirements", ISO 2631-1:1997, International Organization for Standardization, Geneva, Switzerland.

International Organization for Standardization (2007), "Bases for design of structures —Serviceability of buildings

and walkways against vibrations", ISO 10137:2007(E), International Organization for Standardization, Geneva, Switzerland.
Isyumov, N. (1993), "Criteria for acceptable wind-induced motion of tall buildings", *Proceedings of the International Conference on Tall Buildings, CTBUH*, Rio de Janeiro, Brazil.
Isyumov, N. (1995), "Motion perception, tolerance and mitigation", *Proceedings of the 5th World Congress of the Council of Tall Buildings and Urban Habitat*, Amsterdam, The Netherlands.
Irwin, A.W. (1979), "Human response to dynamic motion of structures", *Struct. Eng.*, **56A**(9), 237-244.
Kanda, J., Tamura, Y. and Fujii, K. (1988), "Probabilistic criteria for human perception of low-frequency horizontal motions", *Proceedings of the Symposium/Workshop on Serviceability of Steel and Composite Structures Proceedings,* Pardubice, Czechoslovaki.
Kareem, A. (1988), "Wind-induced response of buildings: A serviceability viewpoint", *Proceedings of the National Engineering Conference, AISC*, Miami Beach, Florida.
Kareem, A., Kijewski, T. and Tamura, Y. (1999), "Mitigation of motions of tall buildings with specific examples of recent applications", *Wind Struct*., **2**(3), 201-251.
Kareem, A. (2008), "Numerical simulation of wind effects: a probabilistic perspective", *J. Wind Eng. Ind. Aerod.,* **96**(10-11), 1472-1497
Kim, Y.C. and Kanda, J. (2008), "Wind response characteristics for habitability of tall buildings in Japan", *Struct. Design Tall Spec. Build.,* **17**(3), 683-718.
Melbourne, W.H. and Cheung, J.C.K. (1988), "Designing for serviceable accelerations in tall buildings", *Proccedings of the 4th International Conference on Tall Buildings*, Hong Kong and Shanghai.
Mendis, P., Ngo, T., Haritos, N., Hira, A., Salami, B. and Cheung, J. (2007), "Wind loading on tall buildings", *E. J. S. E.,* Special issue: 41-54.
NBCC (2005), National Building Code of Canada, Part 4 Structural Design, Commentary 1, Wind Load Effects.
Pozos-Estrada, A., Hong, H.P. and Galsworthy, J.K. (2010), "Serviceability design factors for wind-sensitive structures",*Can. J. Civil Eng.*, **37**(5), 728-738.
Reed, J.W. (1971), "Wind induced motion and human discomfort in tall buildings", Research Report No. 71-42, M. I. T., Cambridge, MA., USA.
Shinosuka, M. (1972), "Monte Carlo solution of structural dynamics", Technical report No. 19, Columbia University, New York.
Simiu, E. and Scanlan, R.H. (1996), *Wind effects on structures*, John Wiley & Sons, Inc., New York.
Tamura, Y. (2003), "Wind Resistant Design of Tall Buildings in Japan", *Proceedings of the 11th International Conference on Wind Engineering, Vol.1, Lubbock*, Texas, USA.
Tamura, Y., Kawana, S., Nakamura, O., Kanda, J. and Nakata, S. (2006), "Evaluation perception of windinduced vibration in buildings", *Proceedings of the Institution of Civil Engineers, Structures & Buildings*, Issue SB5, October.
Vanderplaats, G.N. (1984), *Numerical optimization techniques for engineering design: with applications*, Graw-Hill, New York, Montreal.
Vickery, B.J., Isyumov, N. and Davenport, A.G. (1983), "The role of damping, mass and stiffness in the reduction of wind effects on structures.", *J. Wind Eng. Ind. Aerod*., **11**, 285-294.
Vickery, B.J., Galsworthy, G.K. and Gerges, R. (2001), "The behaviour of simple non-linear tuned mass dampers", *Proceedings of the 6th World Congress of the Council on Tall Buildings and Urban Habitat*, Melbourne, Australia.
Warburton, G. (1982), "Optimum absorber parameters for various combinations of response and excitation parameters", *Earthq. Eng. Struct. D*., **10**(3), 381-401.

CC